AWARD NUMBER: W81XWH-13-1-0494

TITLE: Tinnitus Multimodal Imaging

PRINCIPAL INVESTIGATOR: Steven Wan Cheung

CONTRACTING ORGANIZATION:

UNIVERSITY OF CALIFORNIA, SAN FRANCISCO
SAN FRANCISCO CA 94103-4249

REPORT DATE: December 2016

TYPE OF REPORT: FINAL

PREPARED FOR: U.S. Army Medical Research and Materiel Command
Fort Detrick, Maryland 21702-5012

REPORT DOCUMENTATION PAGE

Form Approved
OMB No. 0704-0188

1. REPORT DATE	2. REPORT TYPE	3. DATES COVERED
December 2016	FINAL	30 October 2013 – 29 September 2016

4. TITLE AND SUBTITLE

Tinnitus Multimodal Imaging

5a. CONTRACT NUMBER

5b. GRANT NUMBER
W81XWH-13-1-0494

5c. PROGRAM ELEMENT NUMBER

6. AUTHOR(S)

Steven W. Cheung
Srikantan S. Nagarajan

E-Mail: Steven.Cheung@ucsf.edu

5d. PROJECT NUMBER

5e. TASK NUMBER

5f. WORK UNIT NUMBER

7. PERFORMING ORGANIZATION NAME(S) AND ADDRESS(ES)

UNIVERSITY OF CALIFORNIA, SAN FRANCISCO
1855 FOLSOM ST STE 425
SAN FRANCISCO CA 94103-4249

8. PERFORMING ORGANIZATION REPORT NUMBER

9. SPONSORING / MONITORING AGENCY NAME(S) AND ADDRESS(ES)

U.S. Army Medical Research and Materiel Command
Fort Detrick, Maryland 21702-5012

10. SPONSOR/MONITOR'S ACRONYM(S)

11. SPONSOR/MONITOR'S REPORT NUMBER(S)

12. DISTRIBUTION / AVAILABILITY STATEMENT

Approved for Public Release; Distribution Unlimited

13. SUPPLEMENTARY NOTES

14. ABSTRACT

Chronic subjective tinnitus is a common auditory perceptual disorder whose neural substrates remain under intense debate. This project successfully executed a multimodal imaging approach to better understand whole brain network connectivity abnormalities. In chronic tinnitus, the following were observed: 1) 3T and 7T resting-state fMRI revealed increased corticostriatal connectivity, between the caudate nucleus and auditory cortices, 2) magnetoencephalographic resting-state functional connectivity imaging (MEGI) showed negative correlation between cognitive performance and alpha coherence in the temporal lobe, 3) MEGI middle latency response to a 1 kHz tone stimuli was significantly delayed, and 4) 7T MR spectroscopic imaging (MRSI) showed a decrease in the GABA/NAA+NA metabolite ratio. Those findings provide further evidence to support the striatal gating model of tinnitus, where dysfunctionally permissive caudate nucleus enables auditory phantoms to reach perceptual awareness. This permits the development of biomarkers to measure tinnitus severity objectively and to monitor tinnitus response to treatment, including basal ganglia neuromodulation.

15. SUBJECT TERMS
Tinnitus; Multimodal Imaging; fMRI; Magnetoencephalographic Imaging; MR Spectroscopic Imaging; Tinnitus Functional Index; Montreal Cognitive Assessment

16. SECURITY CLASSIFICATION OF:			17. LIMITATION OF ABSTRACT	18. NUMBER OF PAGES	19a. NAME OF RESPONSIBLE PERSON
a. REPORT	b. ABSTRACT	c. THIS PAGE			USAMRMC
Unclassified	Unclassified	Unclassified	Unclassified	30	19b. TELEPHONE NUMBER *(include area code)*

Table of Contents

1. INTRODUCTION:

The overall objective of this research project is to test specific predictions that emerge from a novel basal ganglia-centric tinnitus model by evaluating functional connectivity of the striatum to related auditory brain structures and of neural oscillations in auditory cortex, neurotransmitter (Glutamate and GABA) expression levels in the striatum and auditory cortex, and morphologic microstructure of the dorsal and ventral striatum, in three human cohorts:

COHORT 1 - mild to moderate high frequency hearing loss with tinnitus
COHORT 2 - mild to moderate high frequency hearing loss without tinnitus
COHORT 3 - normal to mild high frequency hearing loss without tinnitus

We executed the study by performing 3T and 7T fMRI, magnetoencephalographic imaging, 7T magnetic resonance spectroscopic imaging, and 7T structural MRI.

2. KEYWORDS:

Tinnitus; Multimodal Imaging; fMRI; Magnetoencephalographic Imaging; MR Spectroscopic Imaging; Tinnitus Functional Index.

3. ACCOMPLISHMENTS:

What were the major goals of the project?

For the entire period of performance, 30 October 2013 through 29 October 2016 the following specific aims were addressed:

Specific aim 1 - assess basal ganglia and auditory cortical functional connectivity in tinnitus and its association with level of distress using resting-state fMRI.

SA1a: To determine if the dorsal striatum has abnormal functional connectivity with auditory cortex in tinnitus.
SA1b: To determine if the ventral striatum has abnormal functional connectivity to limbic structures that is related to tinnitus distress.

This aim is 95% complete. Our first manuscript, ‘Increased striatal functional connectivity with auditory cortex in tinnitus,’ has been published in Frontiers in Human Neuroscience (see Appendix). Our second manuscript is in progress.

Specific aim 2 - examine the profile of functional connectivity of auditory cortical oscillations with the rest of the brain in tinnitus using MEGI.

SA2a: To determine if functional connectivity relationships of neural oscillations in auditory cortex are abnormal in tinnitus.

This aim is 95% complete. We have finalized analyses (see accomplishment below) and are preparing two manuscripts.

Specific aim 3 - assess the balance of neurotransmitter levels of the basal ganglia and auditory cortex using MRSI and the microstructure of the basal ganglia using structural MRI in tinnitus.

SA3a: To determine if the striatum and auditory cortex have an abnormal balance of excitation and inhibition in tinnitus by measuring GABA and Glutamate levels.
SA3b: To determine if the microstructure of the dorsal or ventral striatum is abnormal in tinnitus.

This aim is 80% complete. We have nearly completed analyses. As this specific aim required development of innovative methods, we plan to perform further data quality checks before finalizing results and preparing manuscripts.

What was accomplished under these goals?

Specific aim 1:

A. We have published one article that compared subjects with chronic tinnitus with subjects without tinnitus using 3T resting-state fMRI. This publication is now accessible from Frontiers in Human Neuroscience (http://dx.doi.org/10.3389/fnhum.2015.00568) and in the Appendix. In this article, we show chronic tinnitus subjects to have increased functional connectivity between the area LC of the caudate nucleus and the auditory cortices. Furthermore, this increased connectivity is specific to area LC, as other seeded locations of the basal ganglia do not have this finding. The reader is referred to the publication for other findings and discussion of implications.

B. We have now completed a more rigorous study that compares chronic tinnitus subjects with mild to moderate high frequency hearing loss (COHORT 1) with

control subjects without tinnitus matched for hearing loss profile (COHORT 2) using high field 7T resting-state fMRI. We confirm increased connectivity between the caudate nucleus and the auditory cortices in tinnitus, providing strong evidence for our corticostriatal model of subjective tinnitus (Figure 1).

Participants

Resting-state fMRI data using 7T resting-state fMRI have been collected from 63 participants across the three cohorts, as well as from 8 healthy controls (no tinnitus, no or mild hearing loss). This includes 29 subjects with tinnitus and hearing loss (COHORT 1), 12 with hearing loss and no tinnitus (COHORT 2) and 13 with tinnitus and no or mild hearing loss (COHORT 3). Data from 6 subjects from the total of 63 were not analyzable, mostly due to inadequate quality.

Methods: Data Acquisition and Analyses

MRI data was acquired using a 7.0T EXCITE scanner (GE Healthcare, Waukesha, WI) installed at the Surbeck Laboratory at UCSF. For each subject, a high-resolution T1-weighted anatomical MRI was acquired (IRSPGR; 160 1mm slices, FOV=256mm, TR=2300ms, TE=2.98ms). Spontaneous fMRI data (eyes closed) was also collected using a gradient echo planar pulse sequence (76 1.8mm slices, TR=4000ms, TE=17ms). Resting-state fMRI data was spatially preprocessed using standard routines (e.g. anatomical segmentation, co-registration, spatial smoothing at 8 FWHM, artifact rejection, spatial normalization) using the CONN toolbox (https://www.nitrc.org/projects/conn/). Functional connectivity analyses (voxel-by-voxel correlations) and group comparisons (voxelwise unpaired t-tests) were also performed using CONN. We examined connections of the left and right caudate regions as defined anatomically from coordinates in the Connectivity of the left and right caudate as defined from whole regions in the Automatic Anatomical Labeling atlas.

Results

In individuals with and without tinnitus, seeded regions of each caudate show reciprocal patterns of connectivity with contralateral striatal structures. When subjects with tinnitus and hearing loss (TIN+HL [COHORT 1]) and subjects with hearing loss alone (HL [COHORT 2]) are compared, both the left and right caudate regions independently show increased ($p<0.005$) resting-state functional connectivity with primary auditory cortex (A1) in the chronic tinnitus group (Figure 1). These findings provide strong evidence for our corticostriatal model of chronic, subjective tinnitus.

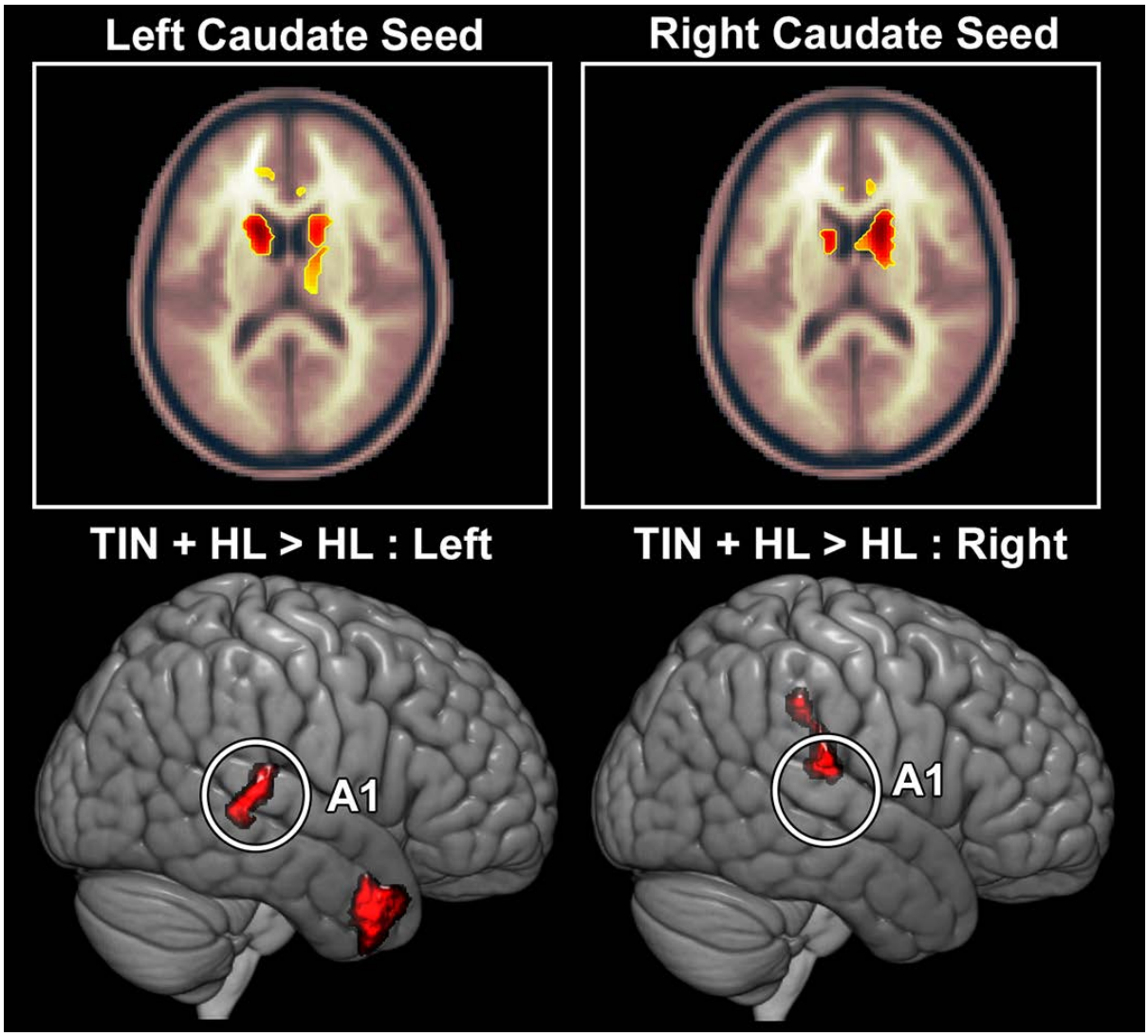

Figure 1. Functional connectivity analysis for resting-state fMRI data collected at 7 Tesla. Top row: Within-group averages for the left and right caudate networks reveal discrete patterns of connections between the basal ganglia bilaterally. Bottom row: Group comparison between subjects with tinnitus and hearing loss (TIN+HL [COHORT 1]) and subjects with hearing loss alone (HL [COHORT 2]). Significant increases in resting-state connectivity between the caudate and primary auditory cortex (A1) are found for both left and right caudate seeds.

Implications

The specificity of these group differences found in the TIN+HL group speak to the utility of high field strength 7T fMRI in identifying functional connectivity change in chronic tinnitus. Specific control for hearing loss profile in this experiment showed the same qualitative results found in lower field strength 3T fMRI, implying robustness of abnormal corticostriatal connectivity in chronic, subjective tinnitus.

Specific aim 2:

A. We have completed data collection and near-final analyses evaluating subjects with tinnitus and hearing loss (TIN+HL [COHORT 1]) using magnetoencephalographic imaging (MEGI) and performing correlational analyses to relate whole brain functional connectivity patterns with cognitive performance levels (Montreal Cognitive Assessment (MoCA)).

Participants

Resting state functional connectivity of alpha-band activity was recorded using magnetoencephalographic imaging (MEGI) to identify regions where patterns of functional connectivity correlated with cognitive performance on the Montreal Cognitive Assessment (MoCA) for 34 tinnitus with hearing loss subjects.

Methods: Data Acquisition and Analyses

Resting state MEGI data were coregistered to a T1 weighted MRI for source space reconstruction. Structural images were acquired on a 3T Siemens MRI scanner at the Neurosciences Imaging Center at UCSF. MEGI data were collected with a sampling rate of 600Hz on a 275-channel whole-head MEG system consisting of 275 axial gradiometers. Three fiducial coils positioned at the nasion and the left and right pre-auricular points were used to localize the position of the head relative to the sensor array. These points were later co-registered to a T1-weighted MRI to generate a head shape. Data collection was optimized to minimize within-session head movements to not exceed 0.5 cm. Ten minutes of continuous recording was collected from each subject lying supine, awake, and with eyes closed. We selected a 60-second epoch of contiguous stationary segment of data for MEG source data analysis. Artifact free segments were selected by using signal amplitudes less than a threshold of 10 pT, and by visually inspecting the sensor data to identify segments without artifacts generated by eyeblinks, saccades, head movements, or muscle contractions.

A 20-mm isotropic grid was used in the sensor space and reconstructed into source space using a minimum-variance adaptive spatial filtering technique. Tomographic reconstructions of the MEG data were generated using a head model based on each subject's structural MRI. Each subject's T1-weighted MRI was spatially normalized to the standard Montreal Neurological Institute template brain using 5 mm voxels. The results of normalization were manually verified in all subjects. A whole brain volume of interest for lead field computation was generated by transforming all points within a spatially normalized MRI that corresponded to locations within the brain and excluded non-cerebral points. For source-space reconstructions, the MEG sensor data were

filtered with a 1-20 Hz fourth-order Butterworth filter. The alpha frequency peak was identified as the greatest power density within the 8–12 Hz range for each subject. Mean alpha power of a 4-Hz window around this peak was used for the subsequent functional connectivity analysis. We computed imaginary coherence, which quantifies the strength of neural oscillations. Global connectivity was computed at each voxel by averaging Fisher's Z-transformed imaginary coherence values of a single voxel with all other voxels in the grid.

MoCA scores were then correlated with global connectivity values at each voxel using the Pearson's correlation. For all voxel-wise functional connectivity correlations with MoCA scores that survived an uncorrected $p < 0.05$, we performed a five voxel cluster correction. Figures 2 and 3 present the activation maps of these correlations between alpha coherence and MoCA scores.

Results

The main findings are negative correlation between the Montreal Cognitive Assessment (MoCA) and alpha coherence of the left temporal gyrus and occipital lobe (Figures 2&3).

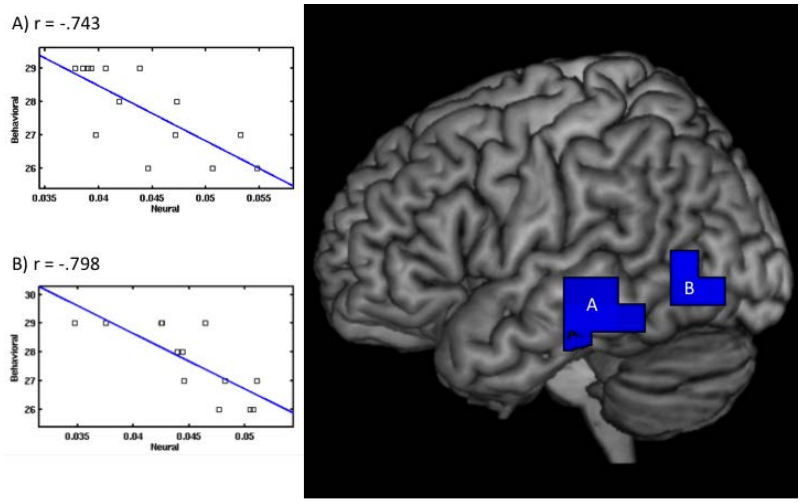

Figure 2. Five voxel cluster corrected activation map and corresponding scatterplots of negative correlation between MoCA and alpha coherence in the left A) middle temporal gyrus and B) occipital lobe. Increased coherence was associated with reduced cognitive performance.

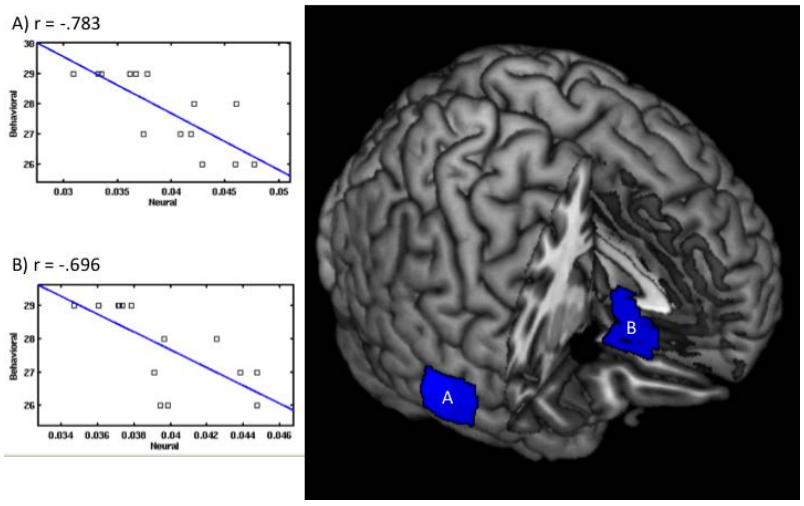

Figure 3. Five voxel cluster corrected activation map and corresponding scatterplots of negative correlation between MoCA and alpha coherence in the right A) middle temporal gyrus and B) mesial anterior cingulate cortex. Increased coherence was associated with reduced cognitive performance.

Implications

These findings suggest that abnormal resting state functional connectivity are associated with impaired cognitive function in chronic tinnitus patients. For further dissection of this provocative finding, the relative contributions of hearing loss and tinnitus will require a separate, dedicated investigation.

B. We have completed data collection and near-final analyses evaluating subjects with tinnitus and hearing loss (TIN+HL [COHORT 1]) and subjects with hearing loss alone (HL [COHORT 2]) using magnetoencephalographic imaging (MEGI) to record auditory evoked field response to a 1 kHz tone.

Participants

The M100 auditory evoked field (AEF) response to a 1 kHz tone was captured using MEGI. Analyzable data were recorded from 31 subjects (24 male, 7 female; mean age = 57 years) with tinnitus and hearing loss (COHORT 1) and 11 tinnitus subjects (4 male, 7 female; mean age = 64 years) with hearing loss alone (COHORT 2). The two study groups were contrasted to evaluate for latency difference for response to a 1 kHz tone.

Methods: Data Acquisition and Analyses

Subjects and controls were presented with 400-millisecond (25 ms ramp up and down) pure-tone stimulus at 1 kHz every 2 seconds for 4 minutes (120 trials) into each hearing ear individually at an intensity level 15 dB to 40 dB above hearing threshold based on comfort. A 275-channel whole-head CTF Omega 2000 system (VSM MedTech) in a

magnetically shielded room with a sampling rate of 600 Hz was used for magnetic field data acquisition. All study participants underwent noncontrast T1-weighted MRIs that were normalized using the Montreal Neurological Institute protocol. MEGI data were then fused to structural MR images.

The source localization algorithm Champagne was used to compute the source strength at each voxel in the brain. MEG sensor data were third-order gradient denoised, detrended, and filtered from 4 to 40 Hz. The 4-Hz high-pass cutoff was used to filter out low-frequency movement-related artifacts, improving detection of the M100. The sensor data for all trials in each condition were averaged. From this average, a three component lead field was generated using the NUTMEG analysis toolbox, which calculates a forward model of sensor activity given a spatially normalized MRI for each subject, coregistered using fiducial markers. The source activity was run through Champagne to compute sensor weights at each 8-mm voxel in the brain. For each subject, weights were extracted for the peak voxel in each hemisphere, determined by activity strength in a window around the M100 response (50-150 ms poststimulus onset). These weights, multiplied by the sensor data, gave the estimation of signal strength at the peak voxel in each hemisphere. We call these signals the ‘‘source space’’ data because they represent the strength of the dipole source that generates a pattern on the sensors. From the source data, the time latency and peak amplitude of the M100 response from the auditory cortex in its immediate environs in each hemisphere and triplanar coordinates were extracted (ipsilateral and contralateral to the auditory stimulus) (Fig.4).

Results

The main finding is abnormally long latency of the M100 peak in response to 1 kHz tone in TIN+HL (COHORT I). Figure 4 shows a representative case in the upper panel and group data for contrast in the lower panel.

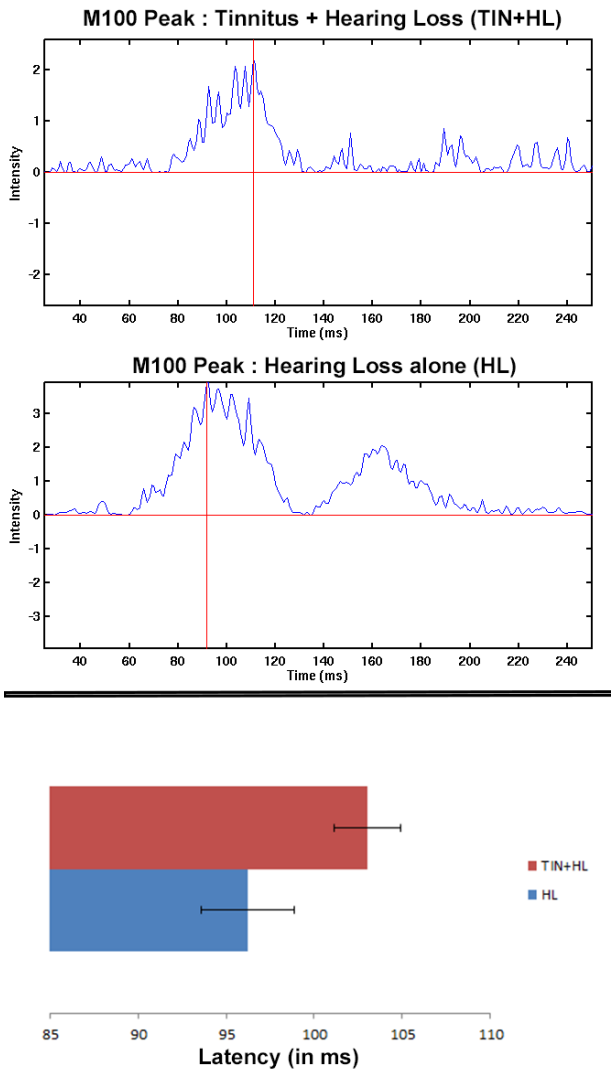

Figure 4. Latency of AEF peaks derived from 1kHz tones presented during MEGI recording sessions in COHORTS 1 & 2: tinnitus with high-frequency hearing loss (TIN+HL) and high-frequency hearing loss alone (HL). Top row: Representative AEF latencies for a single TIN+HL subject and HL subject from source localizations over primary auditory cortex. Bottom row: AEF latencies averaged across the left and right ears for TIN+HL (COHORT 1 in red) and HL (COHORT 2 in blue). TIN+HL show longer AEF latencies when compared to HL alone ($p<0.05$), indicating chronic tinnitus is associated with delayed sound processing in auditory cortex.

Implications

These findings suggest that chronic tinnitus is associated with a longer response latency to a 1 kHz tone. The immediate implications are unclear at this time. This finding may be specific to mild-to-moderate hearing loss, so other matched hearing loss contrast experiments will be required to evaluate this more thoroughly. If proven to be a robust finding across other hearing loss patterns, then abnormally long M100 latency may be a useful biomarker to detect chronic tinnitus objectively.

Specific aim 3:

We have been collecting GABA MR-Spectroscopy data in chronic tinnitus and control subjects using 7T MRI. We have been refining our methods for GABA concentration determination in caudate nucleus and auditory cortex. We have also collected high-resolution 7T structural MRI data that enables us to perform quantitative morphometric analyses.

Participants

Magnetic resonance spectroscopic imaging (MRSI) data was acquired at 7T from a net 57 analyzable participants across the 3 cohorts and an additional cohort of normal, healthy controls.

Methods: Data Acquisition and Analyses

MRSI data was acquired using a 32-channel receive-only array with a volume-transit head coil on a GE 7T MR950 scanner (GE Healthcare, Waukesha, WI). For the single-voxel MRSI, the scanner's coil was used to excite all the ^{1}H signals in a single 2.0 x 2.0 x 2.0 cm^3 voxel seed. GABA detection was achieved by applying a frequency-selective inversion pulse that avoids excitation of the GAA C-3 peak at 1.9 ppm over alternating scans. Four seeds were placed, both left and right Heschl's gyrus (primary auditory cortex; A1) and in the anterior portion of the left and right caudate (caudate head, CH).

Results

Metabolite ratios (GABA/NAA+NA) from left and right CH seeds in patients with tinnitus and hearing loss (COHORT 1) versus patients with hearing loss and no tinnitus (COHORT 2) are presented in Figure 5. Preliminary analysis reveals a more restricted distribution of (GABA/NAA+NA) metabolite ratios in the basal ganglia for the patients with chronic tinnitus (TIN+HL [COHORT 1]) compared to hearing loss matched controls (TIN+HL [COHORT]). COHORT 1 (Figure 5, red) has significantly reduced ($p<0.05$) GABA concentration.

Implications

While further data quality checks are still required before finalizing results and preparing manuscripts, this alteration in GABA expression may be a neurochemical marker of a dysfunctionally permissive dorsal striatal gate in chronic tinnitus. If this assertion will be validated in replication studies, then neurochemical response monitoring of tinnitus treatments may be possible.

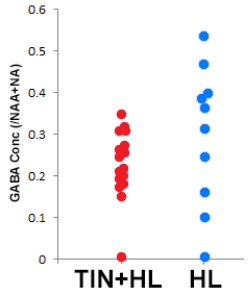

Figure 5. Metabolite ratios (GABA/NAA+NA) collected using 7T MR spectroscopy for seeds placed in the left and right basal ganglia for subjects with chronic tinnitus and hearing loss (TIN+HL, COHORT 1 in red) and hearing loss only (HL, COHORT 2 in blue). GABA/NAA+NA ratio is reduced in the TIN+HL (COHORT 1). GABA concentration alteration may be a neurochemical marker of a dysfunctionally permissive dorsal striatal gate in chronic tinnitus.

What opportunities for training and professional development has the project provided?

The project has provided training and professional development for several members of the study team. Two research associates, Ms. Danielle Mizuiri and Ms. Avery Garrett have been engaged in maximizing subject recruitment and optimizing imaging data collection (MRI and MEGI). We have also trained a senior audiologist (Dr. Jennifer Henderson-Sabes, UCSF) and (Dr. Jolie Chang, Assistant Professor, UCSF) on tinnitus imaging research. Dr. Chang was awarded a Junior Faculty Development Award from the Triological Society to support MEGI studies on hearing disorders. Two new postdoctoral junior scientists have been trained on fMRI, MRSI and MEGI data acquisition and analysis. Dr. Leighton Hinkley is a junior scientist at UCSF who has been leading the analysis of resting-state fMRI data in 3T and 7T scanners. Dr. Yan Li is a staff scientist who has refined MR acquisition sequences for GABA-MRSI in 7T MR scanners. Dr. Carly Demopoulos is a postdoctoral fellow who is leading the analysis of resting-state MEGI. She is also a certified neuropsychologist who is involved in screening and behavioral assessment of all study subjects. She is transiting to become an independent junior scientist at UCSF. All junior scientists work closely with each other and with postdoctoral fellows on data integration across multiple imaging modalities and behavioral assessments. All team members have been supervised by the PI and co-Investigator, Dr. Srikantan Nagarajan, to ensure scientific rigor. The study team holds monthly meetings to assess recruitment status, imaging results, and information dissemination. There are weekly seminars and journal clubs to enrich intellectual development.

How were the results disseminated to communities of interest?

Our first paper has been published in Frontiers in Human Neuroscience, an open access journal. All communities interested in tinnitus will have access to the article. We are planning to submit 7T fMRI, MEGI, and MRSI manuscripts by winter 2017. As we publish results from this project, team members will travel to international conferences to disseminate information.

What do you plan to do during the next reporting period to accomplish the goals?

This the final report. We plan to propose innovative experiments for funding consideration to federal agencies that will extend findings and evaluate biomarkers discovered from this study.

4. IMPACT:

What was the impact on the development of the principal discipline(s) of the project?

Our scientific findings strongly support the striatal gating model for chronic tinnitus. This permits the development of biomarkers to measure tinnitus severity objectively and to monitor tinnitus response to treatment, including basal ganglia neuromodulation.

What was the impact on other disciplines?

These findings have potential impact on other phantom disorders, such as phantom limb pain.

What was the impact on technology transfer?

There is potential that our protocol using multimodal imaging that includes resting-state fMRI, MEGI, and spectroscopic MRI could become an objective diagnostic tool for detecting and monitoring of tinnitus, and other phantom disorders. There is no specific technology for transfer at this time.

What was the impact on society beyond science and technology?

The striatal gating hypothesis has profound implications on the very essence of conscious experience. If further validated, it has potential to revolutionize our concept of external and internal perceptual realities.

5. CHANGES/PROBLEMS:

Changes in approach and reasons for change:

Nothing to report.

Actual or anticipated problems or delays and actions or plans to resolve them:

Recruitment of Veterans proved challenging. We encountered a surprisingly high occurence of Veterans with disqualifying factors: moderate or more severe PTSD, metal in the head, and cardiac stents (7T fMRI and 7T MR spectroscopic imaging contraindicated). In view of the high incidence of disqualifying PTSD, a separate dedicated study will be required to address tinnitus with comorbid PTSD. Findings from this study will provide important background information to design future experiments.

Changes that had a significant impact on expenditures:

Nothing to report.

Significant changes in use or care of human subjects, vertebrate animals, biohazards, and/or select agents:

Nothing to report.

Significant changes in use or care of human subjects

Nothing to report.

Significant changes in use or care of vertebrate animals

Nothing to report.

Significant changes in use of biohazards and/or select agents

Nothing to report.

6. PRODUCTS:

Publications, conference papers, and presentations

Hinkley LB, Mizuiri D, Hong OS, Nagarajan SS, and Cheung SW (2015) Increased striatal functional connectivity with auditory cortex in tinnitus. Front Hum Neurosci 9:568. doi:10.3389/fnhum.2015.00568.

Henderson-Sabes J et al (2016) Tinnitus Imaging. 33rd World Congress of Audiology, Vancouver, Canada.

Cheung SW (2016) Striatal Gating of Auditory Phantoms. American Auditory Society Annual Meeting, Scottsdale, AZ.

7. PARTICIPANTS & OTHER COLLABORATING ORGANIZATIONS

What individuals have worked on the project?

Name:	Steven W. Cheung
Project Role:	PI
Researcher Identifier (e.g. ORCID ID):	
Nearest person month worked:	1.74
Contribution to Project:	Dr. Cheung supervised all aspects of the study. He is actively engaged in audiological and imaging activities associated with this project. Dr. Cheung will jointly analyze data and prepare manuscripts with the research team. Dr. Cheung co-discovered area LC, the dorsal striatal structure hypothesized to be important in tinnitus awareness.

Name:	Srikantan S. Nagarajan
Project Role:	Co-PI
Researcher Identifier (e.g. ORCID ID):	
Nearest person month worked:	1.98
Contribution to Project:	Dr. Nagarajan supervises training of postdoctoral fellows to analyze resting-state MEGI, fMRI and MRSI data. Dr. Nagarajan is Director of the UCSF Biomagnetic Laboratiory and is very experienced in functional connectivity imaging studies in humans.

Name:	Caroline R. Belkoura
Project Role:	Co-Investigator
Researcher Identifier (e.g. ORCID ID):	
Nearest person month worked:	1.20
Contribution to Project:	Dr. Belboura characterizes subjects neuropsychologically. She is an experienced neuropsychologist with specific expertise in performing neurocognitive evaluations. Dr. Racine performs, scores, analyzes, and interprets all neuropsychological tests.

Name:	Carly Demopoulos
Project Role:	Postdoctoral Fellow
Researcher Identifier (e.g. ORCID ID):	
Nearest person month worked:	6.0
Contribution to Project:	Dr. Demopoulos is a postdoctoral fellow and a certified neuropsychologist who is involved in screening and behavioral assessment of all study subjects. She leads the analysis of resting-state MEGI.

Name:	Leighton B. Hinkley
Project Role:	Postdoctoral Fellow
Researcher Identifier (e.g. ORCID ID):	
Nearest person month worked:	6.0
Contribution to Project:	Dr. Hinkley is a junior scientist. He leads the analysis of resting-state fMRI.

Name:	Danielle Mizuiri
Project Role:	Study Coordinator
Researcher Identifier (e.g. ORCID ID):	
Nearest person month worked:	6.0
Contribution to Project:	IRB management, subject recruitment, and imaging data collection (MRI and MEGI).

Name:	Avery Garrett
Project Role:	Study Coordinator
Researcher Identifier (e.g. ORCID ID):	
Nearest person month worked:	6.0
Contribution to Project:	Along with Ms. Mizuiri, Ms. Garrett is engaged in IRB management, subject recruitment, and imaging data collection (MRI and MEGI).

Has there been a change in the active other support of the PD/PI(s) or senior/key personnel since the last reporting period?

Nothing to report.

What other organizations were involved as partners?

Nothing to report.

8. SPECIAL REPORTING REQUIREMENTS:

Not applicable.

9. APPENDICES:

See attachment.

frontiers in Human Neuroscience

ORIGINAL RESEARCH
published: 28 October 2015
doi: 10.3389/fnhum.2015.00568

Increased striatal functional connectivity with auditory cortex in tinnitus

Leighton B. Hinkley[1], Danielle Mizuiri[1], OiSaeng Hong[2], Srikantan S. Nagarajan[1,3] and Steven W. Cheung[3,4]**

[1] Department of Radiology and Biomedical Imaging, University of California at San Francisco, San Francisco, CA, USA, [2] Department of Community Health Systems, School of Nursing, University of California at San Francisco, San Francisco, CA, USA, [3] Department of Otolaryngology-Head and Neck Surgery, University of California at San Francisco, San Francisco, CA, USA, [4] Surgical Services, San Francisco Veterans Affairs Medical Center, San Francisco, CA, USA

Tinnitus is a common auditory perceptual disorder whose neural substrates are under intense debate. One physiologically based model posits the dorsal striatum to play a key role in gating auditory phantoms to perceptual awareness. Here, we directly test this model along with the roles of auditory and auditory-limbic networks in tinnitus non-invasively by comparing resting-state fMRI functional connectivity patterns in chronic tinnitus patients against matched control subjects without hearing loss. We assess resting-state functional connectivity of the caudate dorsal striatum (area LC), caudate head (CH), nucleus accumbens (NA), and primary auditory cortex (A1) to determine patterns of abnormal connectivity. In chronic tinnitus, increases in ipsilateral striatal–auditory cortical connectivity are found consistently only in area LC. Other patterns of increased connectivity are as follows: (1) right striatal area LC, A1, CH, and NA with parietal cortex, (2) left and right CHs with dorsal pre-frontal cortex, (3) NA and A1 with cerebellum, hippocampus, visual and ventral pre-frontal cortex. Those findings provide further support for a striatal gating model of tinnitus, where dysfunctionally permissive area LC enables auditory phantoms to reach perceptual awareness.

Keywords: resting-state fMRI, tinnitus, striatum, auditory cortex, functional connectivity

OPEN ACCESS

Edited by:
John J. Foxe, Albert Einstein College of Medicine, USA

Reviewed by:
Nathan Weisz, University of Trento, Italy
Berthold Langguth, University of Regensburg, Germany
Agnès Job, IRBA-Biomedical Research Institute of the Army, France

****Correspondence:***
Steven W. Cheung
steven.cheung@ucsf.edu;
Srikantan S. Nagarajan
sri@ucsf.edu

Received: *08 April 2015*
Accepted: *28 September 2015*
Published: *28 October 2015*

Citation:
Hinkley LB, Mizuiri D, Hong O, Nagarajan SS and Cheung SW (2015) Increased striatal functional connectivity with auditory cortex in tinnitus. Front. Hum. Neurosci. 9:568. doi: 10.3389/fnhum.2015.00568

INTRODUCTION

Tinnitus is a common perceptual disorder of auditory phantoms where peripheral audiometric hearing loss (HL) profiles alone cannot help clinicians to distinguish between patients who merely experience tinnitus from those who suffer from tinnitus (Coles, 1984; Tsai et al., 2012). Central auditory system hypotheses of tinnitus genesis have been proposed to account for the discrepancy between audiometric profiles and tinnitus perceptual attributes, including lemniscal system hyperactivity (Chen and Jastreboff, 1995; Norena and Eggermont, 2003; Kaltenbach, 2006), tonotopic map plasticity (Komiya and Eggermont, 2000; Syka, 2002; Roberts et al., 2010) and thalamocortical dysrhythmia (Llinas et al., 1999; Weisz et al., 2007) in frequencies including gamma (van der Loo et al., 2009; De Ridder et al., 2011). While those oscillatory (Sedley et al., 2012) and network (Husain, 2007) state models may ultimately prove to be requisite neurophysiological substrates underlying tinnitus, they do not address mechanisms of tinnitus awareness.

A recent development is the striatal gating model (Larson and Cheung, 2012), which hypothesizes the caudate nucleus to act as a gating mechanism for tinnitus awareness.

The striatal gating model is physiologically based, motivated by electrical stimulation experiments in dorsal striatal area LC, located at the junction of the head and body of the caudate nucleus, on awake and interactive humans. Direct stimulation of area LC during deep brain stimulation (DBS) surgery in movement disorders patients with comorbid chronic tinnitus modulates auditory phantom loudness (Cheung and Larson, 2010) and triggers auditory phantom percepts in HL patients without tinnitus (Larson and Cheung, 2012). Furthermore, vascular infarction of area LC results in enduring tinnitus loudness suppression (Larson and Cheung, 2013). According to this model, dysfunctional corticostriatal connections between the dorsal striatum and auditory cortex act as a pathway for auditory phantom representations to reach perceptual awareness. The normally restrictive dorsal striatum becomes pathologically permissive in chronic tinnitus. Although the physiological mechanisms are not clear, it has been proposed that alteration in the balance of excitation and inhibition either within the caudate or in its connections to auditory cortex modulates this permissiveness (Calabresi et al., 2000; Goubard et al., 2011). The striatal gating model is complementary to other central nervous system hypotheses, including those that posit tinnitus is primarily an expectation mismatch within the auditory system (primary auditory cortex (A1); Eggermont and Roberts, 2004; Roberts et al., 2013) or is driven by abnormal auditory-limbic interactions [i.e., nucleus accumbens (NA); Leaver et al., 2011; Seydell-Greenwald et al., 2012]. While invasive direct electrical stimulation studies of the dorsal striatum in movement disorder patients with comorbid tinnitus provide support for a causal role of the basal ganglia in auditory phantom perception, to date no non-invasive neuroimaging study has directly tested the physiologically based striatal gating model in the more common subpopulation of chronic tinnitus patients without movement disorder.

Here, we test the tinnitus striatal gating model directly using seeded coherence of resting-state fMRI on a cohort of chronic, constant tinnitus patients accounted for HL and a cohort of matched control individuals without tinnitus and without HL. Prior non-invasive studies of neuroanatomical connectivity and task-induced activation in the brain have provided evidence for alterations in neural structure and function in tinnitus, but only a handful have examined coherent activity in the brain at resting-state using EEG or fMRI (Vanneste et al., 2011; Kim et al., 2012; Maudoux et al., 2012a,b, Schmidt et al., 2013, Chen et al., 2014, 2015; Davies et al., 2014; Husain and Schmidt, 2014; Vanneste and De Ridder, 2015). None have directly assessed what roles striatal sub-divisions may play in auditory phantom perception. If area LC plays a prominent role in blocking phantom percepts and this mechanism breaks down in tinnitus, then alterations in resting-state functional connectivity should be observed between this structure and auditory cortical fields. Changes in resting-state connectivity for dorsal striatal area LC should be functionally distinct from other striatal sub-divisions and cortical structures involved in auditory perception. We hypothesize that in chronic tinnitus, abnormal functional connectivity between area LC and auditory cortices will be distinct from neighboring fields in the striatum.

MATERIALS AND METHODS

Participants

Fifteen patients (**Table 1**) with chronic, constant tinnitus (TIN) aged 30–63 years (M_{age} = 53.5 years, SD = 13; 3 females) were

TABLE 1 | Demographic descriptions of subjects with chronic tinnitus.

				Audiometric data						
SID	**Age**	**Gender**	**Handed**	**Left low**	**Left high**	**Right low**	**Right high**	**Rating**	**Tinnitus localization**	**THI**
TIN 001	45	Male	Right	28	80	30	80	5	Right and left ears	78
TIN 002	40	Male	Right	10	21	3	23	1	Right and left ears	48
TIN 003	41	Female	Right	48	52	20	8	3	Left ear	14
TIN 004	29	Male	Right	5	8	48	48	3	Right ear	34
TIN 005	63	Male	Right	18	27	22	40	2	Right and left ears	18
TIN 006	69	Male	Right	40	68	30	67	4	Right and left ears	36
TIN 007	45	Female	Right	10	38	3	60	4	Right ear	35
TIN 008	40	Female	Right	22	12	73	50	5	Right ear	36
TIN 009	66	Male	Right	28	83	20	72	5	Right and left ears	52
TIN 010	67	Male	Right	38	60	28	60	4	Right and left ears	32
TIN 011	69	Male	Right	27	50	25	45	3	Right and left ears	44
TIN 012	*55*	Male	Right	8	20	8	23	1	Right and left ears	86
TIN 013	52	Male	Right	7	40	7	30	2	Left ear	22
TIN 014	63	Male	Right	12	42	12	37	3	Right and left ears	12
TIN 015	37	Male	Right	67	72	8	12	5	Left ear	38

Descriptors include age, gender, handedness, hearing profiles in the low and high frequency bands for the left and right ears, HL rating of the poorer frequency band and ear, location of tinnitus, and Tinnitus Handicap Inventory (THI) scores. HL rating (Rating): 1, normal to slight; 2, mild; 3, moderate loss; 4, moderately severe loss; 5, severe loss; 6, profound loss.

recruited from Otolaryngology and Audiology clinics affiliated with the University of California, San Francisco (UCSF). All patients underwent standard clinical audiometry to measure pure tone thresholds and completed the Tinnitus Handicap Inventory (THI; Newman et al., 1996) to assess tinnitus severity. Pure tone audiometric thresholds for low (0.5, 1.0, and 2.0 kHz) and high (4.0, 6.0, and 8.0 kHz) frequency bands were averaged separately to assess HL degree. HL rating was determined by the poorer ear, irrespective of frequency band. The Clark (1981) HL degree scale was adapted to construct the following rating measure: 1 (–10–25 dB), 2 (26–40 dB), 3 (41–55), 4 (56–70 dB), 5 (71–90 dB), and 6 (90+ dB). This metric was used as a covariate in subsequent analysis to account for variability in HL levels within the chronic tinnitus cohort. In addition, 15 healthy control (CON) participants without tinnitus or HL (HL = 1) were recruited from the greater San Francisco Bay Area, matched for age (M_{age}=57 years, SD = 12) and gender, but not for HL. All participants gave written informed consent following explanation of study procedures that were approved by the UCSF Committee on Human Research. All experiments were conducted in accordance with the Declaration of Helsinki.

MRI Acquisition

MRI data was acquired using a 3.0T Siemens Trio (Siemens, Erlangen, Germany) at the UCSF Neuroscience Imaging Center (NIC). For each subject, a high-resolution anatomical MRI was acquired (MPRAGE; 160 1 mm slices, FOV = 256 mm, TR = 2300 ms, TE = 2.98 ms). Eight minutes (240 repetitions) of spontaneous fMRI data was collected (supine position, eyes closed) with a gradient echo-planar imaging (EPI) sequence (38 3.0 mm × 3.0 mm × 3.0 mm slides, TR = 2000 ms, TE = 28 ms).

Data Preprocessing

Resting-state fMRI data was spatially pre-processed and EPI images were spatially realigned to a mean image and coregistered with the T1 image for each individual subject using SPM8[1]. All T1 images were segmented into gray and white matter images and spatially normalized to the MNI template (3 mm isotropic voxels) using the DARTEL toolbox in SPM8 (Ashburner, 2007). Combined transformations to the MNI template were then applied to each realigned EPI image, and those images were subsequently smoothed using a Gaussian kernel with an 8 mm full width at half maximum. After normalization of the EPI images, data from all voxels were linearly detrended and bandpass filtered (second-order Butterworth; 0.01–0.08 Hz) to minimize the effect of physiological artifacts on the resting-state signal. Subsequent functional connectivity analyses were confined to a mask of gray matter voxels from the segmented MNI template using custom-built tools.

Seed Definition

Seed regions were generated using the MarsBar Matlab toolbox[2]. A 5 mm radius sphere was centered on a region of interest (ROI) in each subject's spatially preprocessed data. Seeds were placed bilaterally in four ROIs: (1) area LC (LC), (2) caudate head (CH), (3) nucleus accumbens (NA), and (4) primary auditory cortex (A1), resulting in a total of eight seed ROIs. Seeds for LC and CH were anatomically defined individually by centering the seed over the region based on that subject's anatomical T1-weighted MRI. The NA seeds were chosen from the anatomical location of the accumbens from the Wake Forest University (WFU) PickAtlas toolbox[3] with the 5 mm sphere placed at the center of that location for every subject. For a particular A1 seed, a mask of the transverse temporal gyrus (TTG) was generated using the WFU PickAtlas. The seed region defined the center of mass. Functional connectivity estimates with the rest of the brain were computed separately for left and right seed ROIs.

Functional Connectivity Analysis and Group Statistics

Functional connectivity between each ROI and the rest of the brain was computed using magnitude coherence (Coh) at low-frequency (<0.08Hz) oscillations of the BOLD signal. Magnitude coherence is a metric that estimates correlation in the frequency domain (see Brillinger, 2001; Muller et al., 2001; Sun et al., 2004; Hinkley et al., 2013). Following spatial and temporal preprocessing of EPI images, coherence estimates were calculated between the time series for each voxel in the seed with all remaining voxels in the brain, producing a single whole-brain coherence map for each seed voxel. Coherence values between each seed voxel with all other voxels in the brain were then Fisher Z-transformed and averaged across all seed voxels to yield a functional connectivity map for that ROI with all other regions in the brain (**Figure 1**). In order to normalize data for between group comparisons, each subject's functional connectivity map was standardized by taking the Fisher Z-transformed average score for each voxel and computing a Z-score across all voxels transformed prior to within-group averaging as well as across-group second-level statistics. Voxelwise comparisons between groups (TIN vs. CON) were performed using analysis of covariance (ANCOVA) with group as a factor, with HL magnitude as a covariate. Corrections for multiple comparisons were performed using a cluster thresholding statistic on the ANCOVA results ($p < 0.0075$, $k = 12$ contiguous voxels).

RESULTS

Connectivity Patterns in Controls

Seed connectivity patterns of those ROIs in control subjects provide reference information for comparisons. **Figure 1** shows significant resting-state functional connectivity patterns of the four ROIs (LC, CH, NA, and A1) in control subjects. Although unique connectivity patterns are evident for each seed, there is considerable overlap for area LC and CH. Left and right LC (**Figures 1A,B**): connections to dorsomedial prefrontal cortex

[1]http://www.fil.ion.ucl.ac.uk/spm/software/spm8/

[2]http://marsbar.sourceforge.net

[3]fmri.wfubmc.edu/software/PickAtlas

(dmPFC) and the insula, and basal ganglia bilaterally. Medial and lateral variations in LC seed locations yield similar patterns of functional connectivity. Left and right CH (**Figures 1C,D**): also shows connections with dmPFC bilaterally and regions of the insula and neighboring structures of the basal ganglia. Left and right NA (**Figures 1E,F**) in the ventral striatum: connections with vmPFC, cerebellum, superior temporal lobe and posterior cingulate cortex bilaterally (lower middle rows). Left and right A1 (**Figures 1G,H**): connections to each other, cerebellum, medial prefrontal structures, including dmPFC and the supplementary motor area (SMA), as well as the cuneus in the occipital lobe.

Tinnitus vs. Control Analyses: Subcortical Seeds

For left and right area LC, there are statistically significant increases in connectivity to the ipsilateral medial temporal gyrus (MTG) and superior temporal gyrus (STG) in the tinnitus

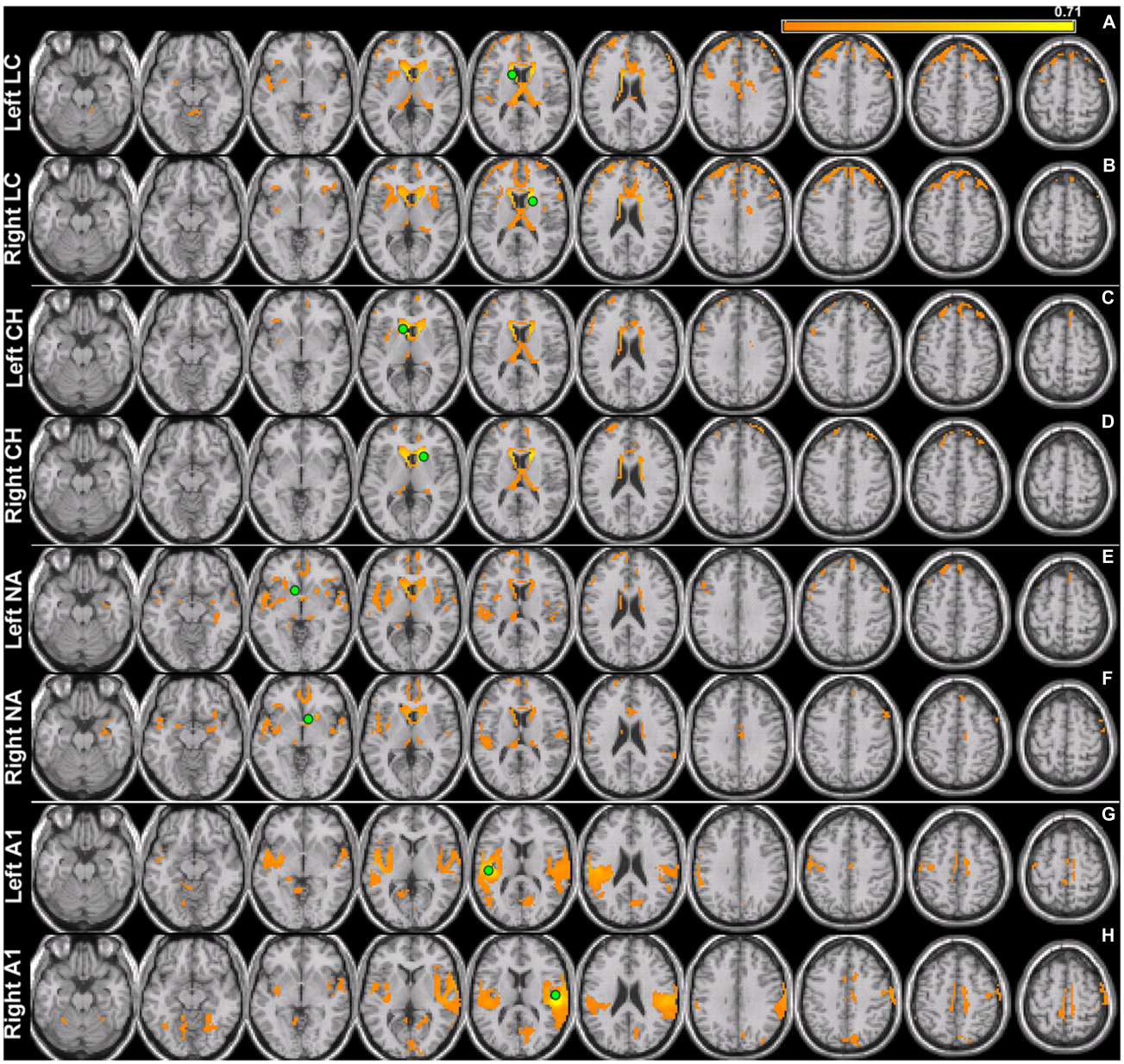

FIGURE 1 | Seed connectivity patterns in control subjects. Seeds (green) are placed in the left and right hemispheres of area LC (LC), caudate head (CH), nucleus accumbens (NA), and primary auditory cortex (A1). Within-subject group averages in the control cohort for the eight seeds that are used to identify resting-state networks show unique connectivity patterns **(A–H)** for each pair. Significant functionally connected voxels include those underneath the marked seed (green circle). All maps are thresholded (80% maximum coherence value) and superimposed on horizontal slices (left-to-right, $z = -22, -12, -2, 5, 15, 25, 32, 42, 52, 62$) of a template brain using MRICro (http://www.mccauslandcenter.sc.edu/mricro/).

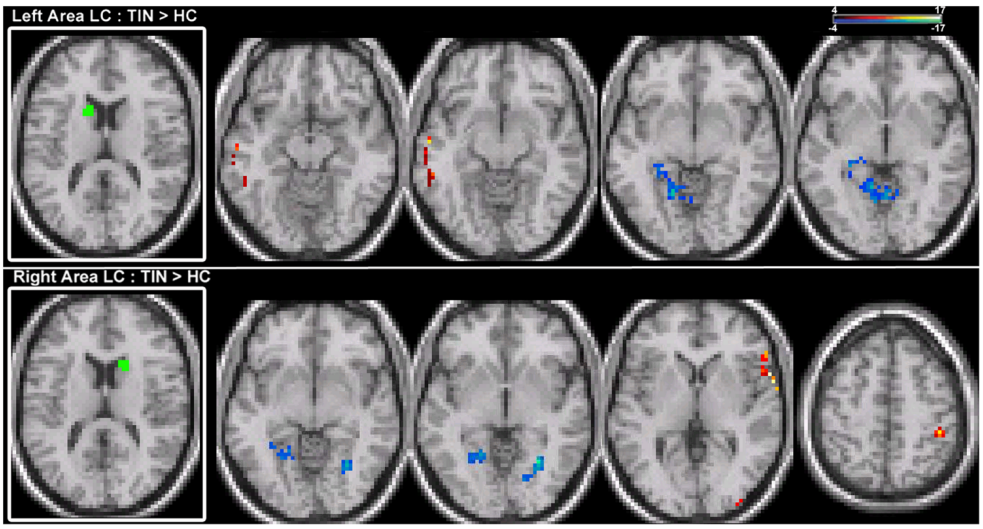

FIGURE 2 | Comparison of tinnitus vs. control: area LC seeds. ANCOVA with hearing loss (HL) as a covariate (thresholded at 0.0075, $k = 12$). **(Top)** Left LC chronic tinnitus resting-state connectivity is increased (red) with auditory regions of the middle temporal gyrus (MTG) and decreased (blue) with lingual gyrus and cerebellum (left-to-right, $z = -14, -13, -8, -6$). **(Bottom)** Right LC chronic tinnitus resting-state connectivity is increased with auditory regions of the superior temporal gyrus (STG), middle occipital gyrus (MOG), and post-central gyrus (PoCG) and decreased with the lingual gyrus (left-to-right, $z = -5, -2, 2, 52$). All coordinates are in MNI space and functional overlays (color bar = F-value) performed using MRICro.

cohort (**Figure 2**; **Table 2**). This increased functional connectivity is still significant after accounting for HL in the poorer ear (**Table 1**). Therefore, connectivity strength of area LC with auditory cortex is abnormally increased in chronic tinnitus. This relationship supports the hypothesis that striatal dysfunction in tinnitus may be the conduit for passage of auditory phantoms that reside in the central auditory system into perceptual awareness. Beyond increased auditory corticostriatal coherence, increased connections are also present between right area LC and the middle occipital gyrus (MOG) and post-central gyrus (PoCG; **Figure 2**; **Table 2**). Decreases in resting-state functional connectivity are identified in connections between both left and right LC and the lingual gyrus and left LC with the cerebellum (**Figure 2**; **Table 2**).

Increases in resting-state coherence with the auditory system are not observed for the CH. Increased connections in the tinnitus cohort are observed for the left and right CH with dorsal pre-frontal cortex in the middle frontal gyrus (MFG) and superior frontal gyrus (SFG) and the right inferior parietal lobe (IPL; **Figure 3**; **Table 2**). Increased connections are also observed for left CH with the contralateral putamen and cingulate cortex (**Figure 3**; **Table 2**). Decreased connections in the tinnitus cohort are observed between right CH with the cerebellum and lingual gyrus (**Figure 3**; **Table 2**).

For connections of the NA, increased connectivity is observed between the right NA and left MTG, but not for the left NA (**Figure 4**; **Table 2**). Both regions show increased connectivity with the left IPL (**Figure 4**; **Table 2**). For left NA, decreased connections are observed with the right STG, cerebellum, and lingual gyrus (**Figure 4**; **Table 2**). For right NA, additional increased connections include left ventral SFG in orbitofrontal cortex, cerebellum, and lingual gyrus (**Figure 4**; **Table 2**). No decreased connections are detected for right NA.

Tinnitus vs. Control Analyses: Cortical Seeds

Seeds placed in left and right A1 exhibit alterations in resting-state functional connectivity. Increases in connectivity are observed between both seeds and left orbital pre-frontal cortex in the SFG and MTG (**Figure 5**; **Table 2**). Furthermore, there are increased connections between left A1 and the anterior STG, cerebellum, right parahippocampal gyrus (PHCG) and lingual gyrus. For right A1, increased connections are also identified with the right MOG and PoCG (**Figure 5**; **Table 2**). Collectively, the tinnitus cohort shows increased connectivity for both seeds between A1 and multiple networks encompassing orbital pre-frontal cortex, the PHCG, cerebellum, and visual cortex.

DISCUSSION

In chronic tinnitus patients adjusted for HL and compared with matched controls, the notable functional connectivity map finding is increased coherence between area LC and ipsilateral auditory cortical fields of the MTG and STG. This consistent, increased coherence is specific to dorsal striatal area LC and is distinct from patterns of connectivity at other sub-divisions of the basal ganglia, including the ventral striatum. Among unique connections of area LC, connections between the basal ganglia and auditory cortex are only discernible in the network for area LC in patients with chronic tinnitus, indicating specificity in the underlying neurobiology of auditory phantom percepts.

TABLE 2 | Target region locations (labels for local maxima and *x, y, z* coordinates), *p*-value at the local maxima and cluster size (in voxels) from a group comparison between patients with chronic tinnitus and matched controls, with hearing loss level as a covariate.

Seed region	Targets : left hemisphere seed	*p*	Targets: right hemisphere seed	*p*	Target network
Area LC	↑ Left MTG (–58, –12, –13)	0.00740	↑ Right STG (62, 82)	0.00046	Auditory
	↓ Left lingual gyrus (–17, –59, –8)	0.00590	↓ Left lingual gyrus (–11, –58, –2)	0.00450	Visual
			↓ Right lingual gyrus (23, –63, –5)	0.00044	
			↑Right MOG (36, –95, 5)	0.00680	
	↓ Left culmen (–14, –49, –6)	0.00660			Cerebellar
			↑ Right PoCG (44, –39, 52)	0.00210	Parietal
Caudate Head			↓ Left culmen (–8, –59, –6)	0.00360	Cerebellar
	↑ Right putamen (20, 7, –11)	0.00126			Basal Ganglia
			↓ Right lingual gyrus (24, –65, –8)	0.00740	Visual
	↑ Right MFG (3, 45, 47)	0.00240	↑ Left SFG (–3, 38, 54)	0.00720	Dorsal Pre-frontal
	↑ Right cingulate (5, 17, 47)	0.00520			Default mode network (DMN)
	↑ Right IPL (41, –40, 53)	0.00076	↑ Right IPL (42, –38, 51)	0.00110	Parietal
Nucleus Accumbens	↓ Right STG (65, –24, –1)	0.00600	↑ Left MTG (–60, –26, –12)	0.00650	Auditory
			↑ Left SFG (–4, 52, –21)	0.00210	Orbital pre-frontal
	↓ Rght culmen (10, –55, 6)	0.00079	↑ LeftPoCb (–12, –76, –23)	0.00400	Cerebellar
	↓ Left lingual gyrus (–16, –55, 7)	0.00220	↑ Left lingual (–25, –76, –12)	0.00120	Visual
	↓ Right lingual gyrus (19, –69, 6)	0.00130			
	↓ Left IPL (–36, –44, 48)	0.00630	↑ Left I PL (–40, –38, 48)	0.00420	Parietal
Primary Auditory Cortex	↑ Right anterior STG (52, 14, –25)	0.00740			Temporal pole
	↑ Left MTG (–65, –34, –6)	0.00730	↑ Left MTG (–60, –34, –7)	0.00740	Auditory
	↑ Left SFG (–6, 56, –21)	0.00210	↑ Left SFG (–6, 55, –21)	0.00230	Orbital pre-frontal
	↑ Left PoCb (–11, –79, –21)	0.00650			Cerebellar
	↑ Right PHCG (27, 3, –13)	0.00210			Hippocampal
	↑ Left lingual gyrus (–29, –82, –11)	0.00330	↑ Right MOG (50, –70, –12)	0.00710	Visual
			↑ Right PoCG (64, –24, 18)	0.00730	Parietal

Target regions for the four different seed regions (area LC, CH, NA, and A1) are shown for each hemisphere. Target regions are organized by the target network shown in the last column. SFG, superior frontal gyrus; IPL, inferior parietal lobe; MTG, middle temporal gyrus; MOG, middle occipital gyrus; PoCG, post-central gyrus; STG, superior temporal gyrus; MFG, middle frontal gyrus; PHCG, parahippocampal gyrus; PoCb, posterior cerebellum.

Those findings provide further support for a basal ganglia-centric model and a potential platform to measure tinnitus objectively.

Increased connectivity of area LC with ipsilateral auditory cortex in chronic tinnitus may be altered by lesioning the dorsal striatum, where vascular insult to area LC causes tinnitus suppression to be more robustly expressed in the ipsilateral ear (Larson and Cheung, 2013). Whereas the dorsal striatum plays an important role in gating auditory phantom representations in auditory cortex for perceptual awareness, functional sub-divisions of the basal ganglia may play separate, but undefined roles in chronic tinnitus. Hyperconnectivity of area LC may be acting as a low-resistance conduit through which auditory phantoms represented in the central auditory system are gated into perceptual awareness. It should be noted that group differences in the connections of area LC to the MTG/STG remain significant following adjustment for HL. ANCOVA results account for HL magnitude by treating it as a covariate in the group analysis. This finding is congruent with the clinical observation that tinnitus severity as assessed by the THI is uncorrelated with the absolute and relative magnitude of HL in the poorer ear (Tsai et al., 2012).

Beyond abnormal basal ganglia connectivity, chronic tinnitus patients also have abnormal patterns of auditory cortical connectivity. A1 has increased coherence with the PHCG, cerebellum, and orbital pre-frontal cortex, a major hub of the default mode network (DMN; Greicius et al., 2003). While not directly related to the striatal gating model, it is possible that increased connectivity between A1 and subregions of the DMN (as well as CH with the DMN) may be related to introspection in this cohort, a function known to be modulated by the DMN (Fransson, 2005). Previous studies have shown that the strength of regional functional connectivity (global cross-correlations of the BOLD signal) for regions of the DMN are related to the amplitude of auditory phantom percepts (Ueyama et al., 2013), though this relationship between A1 and the DMN is not replicated in the current study.

Neuroanatomical tracer studies of connections between the striatum with surrounding cortical fields in the temporal lobe

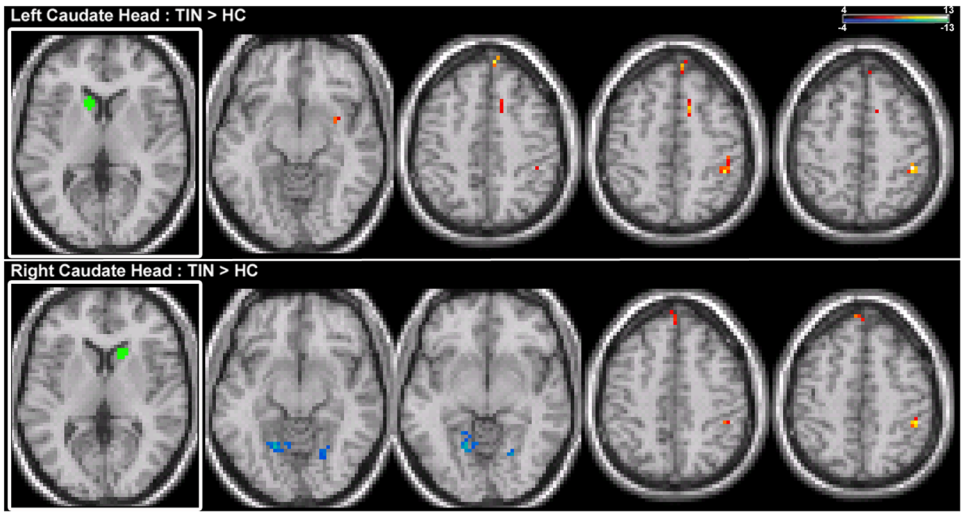

FIGURE 3 | Comparison of tinnitus vs. control: CH seeds. (Top) Left CH chronic tinnitus resting-state connectivity is increased with the putamen, middle frontal gyrus (MFG), cingulate, and inferior parietal lobe (IPL) of the right hemisphere (left-to-right, $z = -11, 46, 48, 53$). **(Bottom)** Right CH chronic tinnitus resting-state connectivity is increased with the left dorsal superior frontal gyrus (SFG) and right IPL and decreased with the cerebellum and lingual gyrus (left-to-right, $z = -8, -6, 51, 54$). Conventions as in **Figure 2**.

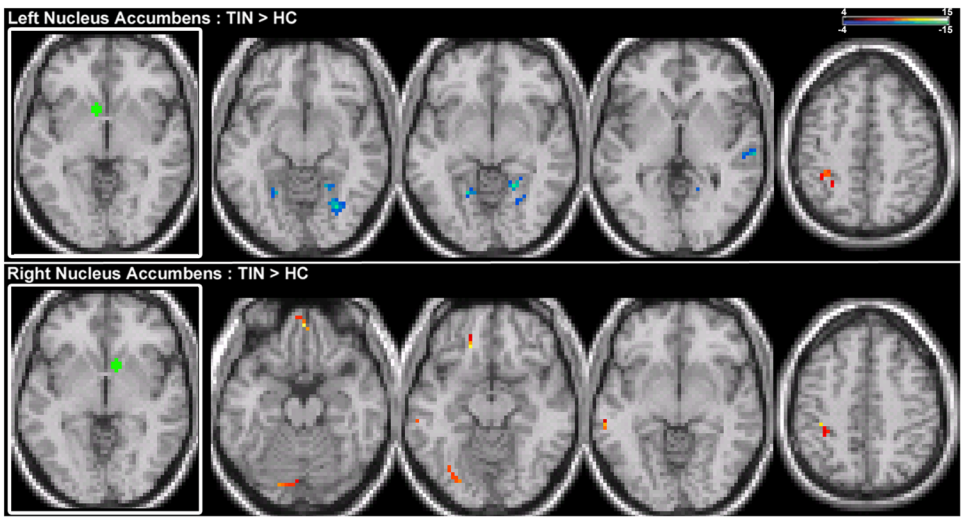

FIGURE 4 | Comparison of tinnitus vs. control: NA seeds. (Top) Left NA chronic tinnitus resting-state connectivity is increased with the left IPL and decreased with the right STG, cerebellum, and lingual gyrus (left-to-right, $z = -11, -6, -2, 48$). **(Bottom)** Right NA chronic tinnitus resting-state connectivity is increased with the left MTG, ventral SFG, cerebellum, lingual gyrus, and IPL (left-to-right, $z = -21, -12, -3, 48$). Conventions as in **Figure 2**.

are remarkable for dorsal striatal connectivity to auditory cortex outside A1 (Reale and Imig, 1983; Selemon and Goldman-Rakic, 1985; Parent and Hazrati, 1995; Yeterian and Pandya, 1998). Besides A1, rostral auditory belt fields connect directly to the caudate in marmoset monkeys (de la Mothe et al., 2006). Similar patterns of connections have been identified in humans using non-invasive neuroimaging studies (Postuma and Dagher, 2006; Robinson et al., 2012). It follows that requisite corticostriatal neural circuitry is in place for dysfunctional striatal connectivity to enable perception of auditory phantoms. Altered auditory corticostriatal connectivity may drive change to a phantom percept network state where connectivity strengths of dense interconnections (Middleton and Strick, 2002) between the striatum and prefrontal cortical fields (dorsolateral, ventrolateral, medial, cingulate) are rebalanced. This notion is supported in the present study by our observations in the tinnitus cohort of increased connectivity with either medial pre-frontal, orbital pre-frontal, or cingulate cortex. However, the clinical correlates of those aberrant striatal–prefrontal connections in tinnitus remain to be defined. Voxelwise correlations with THI scores in the tinnitus cohort were insignificant when corrected for multiple comparisons. Future studies will need to investigate, in larger

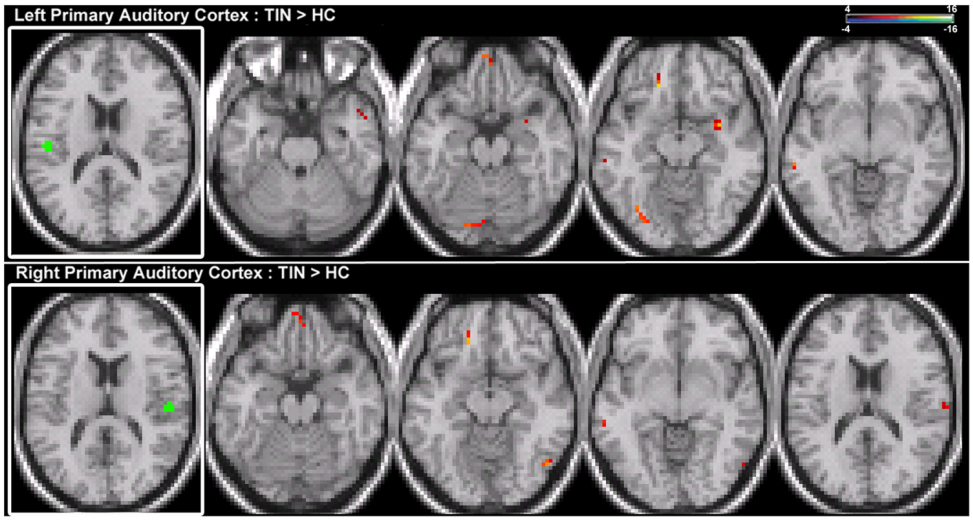

FIGURE 5 | Comparison of tinnitus vs. control: primary auditory cortex seeds. (Top) Left primary auditory cortex (A1) chronic tinnitus resting-state connectivity is increased with the anterior STG, MTG, ventral SFG, cerebellum, parahippocampal gyrus (PHCG), and lingual gyrus (left-to-right, $z = -21, -13, -11, -6$). **(Bottom)** Right A1 chronic tinnitus resting-state connectivity is increased with the MTG, ventral SFG, MOG, and PoCG (left-to-right, $z = -21, -18, -12, 17$). Conventions as in **Figure 2**.

cohorts, relationships between tinnitus variables (such as distress, loudness) with patterns of connectivity to isolate functional substrates of pathologic networks. Functional analysis can be complemented with anatomical measurements. For example, volumetric analysis shows reduced gray matter in vmPFC where the magnitude of reduction is correlated with tinnitus loudness (Leaver et al., 2012).

This first study to evaluate directly connectivity patterns of striatum sub-divisions in chronic tinnitus validates the striatal gating model and confirms findings of prior resting-state EEG and fMRI studies (Vanneste et al., 2011; Maudoux et al., 2012a,b). Increases in functional connectivity with the PHCG are also observed in EEG studies of tinnitus, particularly in responders to transcranial stimulation (Vanneste et al., 2011). Similar to the patterns of resting-state functional connectivity we observe here, coherent oscillations between auditory cortex and the posterior cingulate are related to tinnitus symptoms (Vanneste and De Ridder, 2015). Studies using Independent Component Analysis on resting-state fMRI data have identified increased, aberrant connectivity of regions including the PHCG and parietal lobe (Maudoux et al., 2012b; Schmidt et al., 2013) and basal ganglia, and NA and cerebellum (Maudoux et al., 2012a,b). Interestingly, a recent study inducing tinnitus pharmacologically (Chen et al., 2015) reports increased connections between auditory cortex and the cerebellum and hippocampal gyrus, in concordance with the present study. Our finding of reduced connectivity in the lingual gyrus is consistent with the observations of Lehner et al. (2014), where reduced gray matter volume correlates with improvement in symptoms following TMS. Increased connections between the auditory network and dmPFC were reported in a small sample of tinnitus patients on a resting-state fMRI study (Kim et al., 2012), but other studies have failed to reproduce this finding (Schmidt et al., 2013; Davies et al., 2014). Heterogeneity among tinnitus cohorts may be contributing to network state variations.

There are several limitations to this study. Our sample size of 15 subjects in the chronic tinnitus cohort is relatively small. While our tinnitus and control cohorts are well matched for gender, age, and handedness, they are not matched for HL. HL is inhomogeneous in the poorer ear (**Table 1**). Tinnitus laterality is bilateral in 8 and unilateral in 7. This study is not sufficiently powered to ascertain whether tinnitus laterality is associated with distinct patterns of corticostriatal connectivity. Despite this heterogeneity, robust group differences manifest as increases in unilateral functional connectivity between area LC and auditory cortex in chronic tinnitus. Future studies on corticostriatal connectivity may address potential confounds by matching HL profiles of the tinnitus and control cohorts (as in Schmidt et al., 2013) or studying tinnitus patients with no HL at all (as in Chen et al., 2014). Larger cohorts can address the extent to which HL and tinnitus laterality impacts coherence in the BOLD signal between regions (Tibbetts et al., 2011; Schmidt et al., 2013), and reduce the likelihood of false positives. Although acquisition parameters in this study provide stability in the signal (Van Dijk et al., 2010) future studies examining longitudinal scale resting-state functional connectivity would require longer acquisition times (Birn et al., 2013). With those next steps, we can start to unravel how alterations in connectivity affect perceptual, attentional, and emotional aspects of tinnitus among subgroups.

In summary, the current work contributes to a growing body of literature examining corticostriatal interactions in tinnitus. A testable hypothesis of the striatal gating model of tinnitus has been assessed using resting-state fMRI. The physiologically

based model derived from awake, interactive humans reporting on tinnitus modulation from direct electrical stimulation of the caudate nucleus predicts abnormal connectivity between area LC and auditory cortex. Results from this study have taken a step forward to validate the striatal gating model.

ACKNOWLEDGMENTS

This work was supported by the Department of Defense (Award W81XWH-13-1-0494 to SC), UCSF Academic Senate Committee (Individual Investigator Grant to SC), and Coleman Memorial and Hearing Research, Inc, endowment funds.

REFERENCES

Ashburner, J. (2007). A fast diffeomorphic image registration algorithm. *Neuroimage* 38, 95–113. doi: 10.1016/j.neuroimage.2007.07.007

Birn, R. M., Molloy, E. K., Patriat, R., Parker, T., Meier, T. B., Kirk, G. R., et al. (2013). The effect of scan length on the reliability of resting-state fMRI connectivity estimates. *Neuroimage* 83, 550–558. doi: 10.1016/j.neuroimage.2013.05.099

Brillinger, D. R. (2001). *Time Series: Data Analysis and Theory*. Philadelphia, PA: Society for Industrial and Applied Mathematics.

Calabresi, P., Centozone, D., Gubellini, P., Marfia, G. A., Pisani, A., Sancesario, G., et al. (2000). Synapic transmission in the striatum: from plasticity to neurodegeneration. *Prog. Neurobiol.* 61, 231–265. doi: 10.1016/S0301-0082(99)00030-1

Chen, G. D., and Jastreboff, P. J. (1995). Salicylate-induced abnormal activity in the inferior colliculus of rats. *Hear. Res.* 82, 158–178. doi: 10.1016/0378-5955(94)00174-O

Chen, Y. C., Li, X., Wang, J., Lu, C. Q., Yang, M., Jiao, Y., et al. (2015). Tinnitus and hyperacusis involve hyperactivity and enhanced connectivity in auditory-limbic-arousal-cerebellar network. *Elife* 12:e06576. doi: 10.7554/eLife.06576

Chen, Y. C., Zhang, J., Li, X. W., Xia, W., Feng, X., Gao, B., et al. (2014). Aberrant spontaneous brain activity in chronic tinnitus patients revealed by resting-state functional MRI. *Neuroimage Clin.* 6, 222–228. doi: 10.1016/j.nicl.2014.09.011

Cheung, S. W., and Larson, P. S. (2010). Tinnitus modulation by deep brain stimulation in locus of caudate neurons (area LC). *Neuroscience* 169, 1768–1778. doi: 10.1016/j.neuroscience.2010.06.007

Clark, J. G. (1981). Uses and abuses of hearing loss classification. *ASHA* 23, 493–500.

Coles, R. R. A. (1984). Epidemiology of tinnitus: (2) Demographic and clinical features. *J. Laryngol. Otol.* 98, 195–202. doi: 10.1017/S175514630009046 6

Davies, J., Gander, P. E., Andrews, M., and Hall, D. A. (2014). Auditory network connectivity in tinnitus patients: a resting-state fMRI study. *Int. J. Audiol.* 53, 192–198. doi: 10.3109/14992027.2013.846482

de la Mothe, L. A., Blumell, S., Kajikawa, Y., and Hackett, T. A. (2006). Cortical connections of the auditory cortex in marmoset monkeys: core and medial belt regions. *J. Comp. Neurol.* 496, 27–71.

De Ridder, D., van der Loo, E., Vanneste, S., Gais, S., Plazier, M., Kovacs, S., et al. (2011). Theta-gamma dysrhythmia and auditory phantom perception. *J. Neurosurg.* 114, 912–921. doi: 10.3171/2010.11.JNS10335

Eggermont, J. J., and Roberts, L. E. (2004). The neuroscience of tinnitus. *Trends Neurosci.* 27, 676–682. doi: 10.1016/j.tins.2004.08.010

Fransson, P. (2005). Spontaneous low-frequency BOLD signal fluctuations: an fMRI investigation of the resting-state default mode of brain function hypothesis. *Hum. Brain Mapp.* 26, 15–29. doi: 10.1002/hbm.20113

Goubard, V., Fino, E., and Venance, L. (2011). Contribution of astrocytic glutamate and GABA uptake to corticostriatal information processing. *J. Physiol.* 589, 2301–2319. doi: 10.1113/jphysiol.2010.203125

Greicius, M. D., Krasnow, B., Reiss, A. L., and Menon, V. (2003). Functional connectivity in the resting brain: a network analysis of the default mode hypothesis. *Proc. Natl. Acad. Sci. U.S.A.* 100, 253–258. doi: 10.1073/pnas.0135058100

Hinkley, L. B., Sekihara, K., Owen, J. P., Westlake, K. P., Byl, N. N., and Nagarajan, S. S. (2013). Complex-value coherence mapping reveals novel abnormal resting-state functional connectivity networks in task-specific focal hand dystonia. *Front. Neurol.* 4:149. doi: 10.3389/fneur.2013.00149

Husain, F. T. (2007). Neural network models of tinnitus. *Prog. Brain Res.* 166, 125–140. doi: 10.1016/S0079-6123(07)66011-7

Husain, F. T., and Schmidt, S. A. (2014). Using resting state functional connectivity to unravel networks of tinnitus. *Hear. Res.* 307, 153–162. doi: 10.1016/j.heares.2013.07.010

Kaltenbach, J. A. (2006). The dorsal cochlear nucleus as a participant in the auditory, attentional and emotional components of tinnitus. *Hear. Res.* 21, 224–234. doi: 10.1016/j.heares.2006.01.002

Kim, J. Y., Kim, Y. H., Lee, S., Seo, J. H., Song, H. J., Cho, J. H., et al. (2012). Alteration of functional connectivity in tinnitus brain revealed by resting-state fMRI? A pilot study. *Int. J. Audiol.* 51, 413–417. doi: 10.3109/14992027.2011.652677

Komiya, H., and Eggermont, J. J. (2000). Spontaneous firing activity of cortical neurons in adult cats with reorganized tonotopic map following pure-tone trauma. *Acta Otolaryngol.* 120, 750–756. doi: 10.1080/0001648007500 00298

Larson, P. S., and Cheung, S. W. (2012). Deep brain stimulation in area LC controllably triggers auditory phantom percepts. *Neurosurgery* 70, 398–406. doi: 10.1227/NEU.0b013e3182320ab5

Larson, P. S., and Cheung, S. W. (2013). A stroke of silence: tinnitus suppression following placement of a deep brain sitmulation electrode with infarction in area LC. *J. Neurosurg.* 118, 192–194. doi: 10.3171/2012.9.JNS12594

Leaver, A. M., Renier, L., Chevillet, M. A., Morgan, S., Kim, H. J., and Rauschecker, J. P. (2011). Dysregulation of limbic and auditory networks in tinnitus. *Neuron* 69, 33–43. doi: 10.1016/j.neuron.2010.12.002

Leaver, A. M., Seydell-Greenwald, A., Turesky, T. K., Morgan, S., Kim, H. J., and Rauschecker, J. P. (2012). Cortico-limbic morphology separates tinnitus from tinnitus distress. *Front. Syst. Neurosci.* 6:21. doi: 10.3389/fnsys.2012.00021

Lehner, A., Langguth, B., Poeppl, T. B., Rupprecht, R., Hajak, G., Landgrebe, M., et al. (2014). Structural brain changes following left temporal low-frequency rTMS in patients with subjective tinnitus. *Neural Plasticity* 2014:132058.

Llinas, R. R., Ribary, U., Jeanmonod, D., Kronberg, E., and Mitra, P. P. (1999). Thalamocortical dysrhythmia: a neurological and neuropsychiatric syndrome characterized by magnetoencephalography. *Proc. Natl. Acad. Sci. U.S.A.* 96, 15222–15227. doi: 10.1073/pnas.96.26.15222

Maudoux, A., Lefebvre, P., Cabay, J. E., Demertzi, A., Vanhaudenhuyse, A., Laureys, S., et al. (2012a). Auditory resting-state network connectivity in tinnitus: a functional MRI study. *PLoS ONE* 7:e36222. doi: 10.1371/journal.pone.0036222

Maudoux, A., Lefebvre, P., Cabay, J. E., Demertzi, A., Vanhaudenhuyse, A., Laureys, S., et al. (2012b). Connectivity graph analysis of the auditory resting state network in tinnitus. *Brain Res.* 1485, 10–21. doi: 10.1016/j.brainres.2012.05.006

Middleton, F. A., and Strick, P. L. (2002). Basal-ganglia 'projections' to the prefrontal cortex of the primate. *Cereb. Cortex* 12, 926–935. doi: 10.1093/cercor/12.9.926

Muller, K., Lohmann, G., Bosch, V., and von Cramon, D. Y. (2001). On multivariate spectral analysis of fMRI time series. *Neuroimage* 14, 347–356. doi: 10.1006/nimg.2001.0804

Newman, C. W., Jacobson, G. P., and Spitzer, J. B. (1996). Development of the tinnitus handicap inventory. *Arch. Otolaryngol. Head Neck Surg.* 122, 143–148. doi: 10.1001/archotol.1996.01890140029007

Norena, A. J., and Eggermont, J. J. (2003). Changes in spontaneous neural activity immediately after an acoustic trauma: implications for neural correlates of tinnitus. *Hear. Res.* 183, 137–153. doi: 10.1016/S0378-5955(03)00225-9

Parent, A., and Hazrati, L. N. (1995). Functional anatomy of the basal ganglia. I. The cortico-basal ganglia-thalamo-cortical loop. *Brain Res. Rev.* 20, 91–127.

Postuma, R. B., and Dagher, A. (2006). Basal ganglia functional connectivity based on a meta-analysis of 126 positron emission tomography and functional

magnetic resonance imaging publications. *Cereb. Cortex* 16, 1508–1521. doi: 10.1093/cercor/bhj088

Reale, R. A., and Imig, T. J. (1983). Auditory cortical field projections to the basal ganglia of the cat. *Neuroscience* 8, 327–334. doi: 10.1016/0306-4522(83)90026-X

Roberts, L. E., Eggermont, J. J., Caspary, D. M., Shore, S. E., Melcher, J. R., and Kaltenbach, J. A. (2010). Ringing ears: the neuroscience of tinnitus. *J. Neurosci.* 30, 14972–14979. doi: 10.1523/JNEUROSCI.4028-10.2010

Roberts, L. E., Husain, F. T., and Eggermont, J. J. (2013). Role of attention in the generation and modulation of tinnitus. *Neurosci. Biobehav. Rev.* 37, 1754–1773. doi: 10.1016/j.neubiorev.2013.07.007

Robinson, J. L., Laird, A. R., Glahn, D. C., Blangero, J., Sanghera, M. K., Pessoa, L., et al. (2012). The functional connectivity of the human caudate: an application of meta-analytic connectivity modeling with behavioral filtering. *Neuroimage* 60, 117–129. doi: 10.1016/j.neuroimage.2011.12.010

Schmidt, S. A., Akrofi, K., Carpenter-Thompson, J. R., and Husain, F. T. (2013). Default mode, dorsal attention and auditory resting state networks exhibit differential functional connectivity in tinnitus and hearing loss. *PLoS ONE* 8:e76488. doi: 10.1371/journal.pone.0076488

Sedley, W., Teki, S., Kumar, S., Barnes, G. R., Bamiou, D. E., and Griffiths, T. D. (2012). Single-subject oscillatory γ responses in tinnitus. *Brain* 135, 3089–3100. doi: 10.1093/brain/aws220

Selemon, L. D., and Goldman-Rakic, P. S. (1985). Longitudinal topography and interdigitation of corticostriatal projections on the rhesus monkey. *J. Neurosci.* 5, 776–794.

Seydell-Greenwald, A., Leaver, A. M., Turesky, T. K., Morgan, S., Kim, H. J., and Rauschecker, J. P. (2012). Functional MRI evidence for a role of ventral prefrontal cortex in tinnitus. *Brain Res.* 1485, 22–39. doi: 10.1016/j.brainres.2012.08.052

Sun, F. T., Miller, L. M., and D'Esposito, M. (2004). Measuring interregional functional connectivity using coherence and partial coherence analyses of fMRI data. *Neuroimage* 21, 647–658. doi: 10.1016/j.neuroimage.2003.09.056

Syka, J. (2002). Plastic changes in the central auditory system after hearing loss, restoration of function, and during learning. *Physiol. Rev.* 82, 601–636. doi: 10.1152/physrev.00002.2002

Tibbetts, K., Ead, B., Umansky, A., Coalson, R., Schlaggar, B. L., Firszt, J. B., et al. (2011). Interregional brain interactions in children with unilateral hearing loss. *Otolaryngol. Head Neck Surg.* 144, 602–611. doi: 10.1177/0194599810394954

Tsai, B. S., Sweetow, R. W., and Cheung, S. W. (2012). Audiometric asymmetry and tinnitus laterality. *Laryngoscope* 122, 1148–1153. doi: 10.1002/lary.23242

Ueyama, T., Donishi, T., Ukai, S., Ikeda, Y., Hotomi, M., Yamanaka, N., et al. (2013). Brain regions responsible for tinnitus distress and loudness: a resting-state fMRI study. *PLoS ONE* 8:e67778. doi: 10.1371/journal.pone.0067778

van der Loo, E., Gais, S., Congedo, M., Vanneste, S., Plazier, M., Menovsky, T., et al. (2009). Tinnitus intensity dependent gamma oscillations of the contralateral auditory cortex. *PLoS ONE* 4:e7396. doi: 10.1371/journal.pone.0007396

Van Dijk, K. R., Hedden, T., Venkataraman, A., Evans, K. C., Lazar, S. W., and Buckner, R. L. (2010). Intrinsic functional connectivity as a tool for human connectomics: theory, properties, and optimization. *J. Neurophysiol.* 103, 297–321. doi: 10.1152/jn.00783.2009

Vanneste, S., and De Ridder, D. (2015). Stress-related functional connectivity changes between auditory cortex and cingulate in tinnitus. *Brain Connect* 5, 371–383. doi: 10.1089/brain.2014.0255

Vanneste, S., Focquaert, F., Van de Heyning, P., and De Ridder, D. (2011). Different resting state brain activity and functional connectivity in patients who respond and not respond to bifrontal tDCS for tinnitus suppression. *Exp. Brain Res.* 210, 217–227. doi: 10.1007/s00221-011-2617-z

Weisz, N., Muller, S., Schlee, W., Dohrmann, K., Hartmann, T., and Elbert, T. (2007). The neural code of auditory phantom perception. *J. Neurosci.* 27, 1479–1484. doi: 10.1523/JNEUROSCI.3711-06.2007

Yeterian, E. H., and Pandya, D. N. (1998). Corticostriatal connections of the superior temporal region in rhesus monkeys. *J. Compar. Neurol.* 399, 384–402.

Conflict of Interest Statement: The authors declare that the research was conducted in the absence of any commercial or financial relationships that could be construed as a potential conflict of interest.